Applied Catalysis B: Environmental 241 (2019) 299–304

Contents lists available at ScienceDirect

Applied Catalysis B: Environmental

journal homepage: www.elsevier.com/locate/apcatb

Formation of silica nanolayer on titania surface by photocatalytic reaction

Hiromasa Nishikiori[a,b,c,*], Shingo Matsunaga[b], Moeko Iwasaki[b], Nobuyuki Zettsu[a,b,c], Mari Yamakawa[a], Ayaka Kikuchi[b], Tomohiko Yamakami[b], Katsuya Teshima[a,b,c]

[a] Department of Materials Chemistry, Faculty of Engineering, Shinshu University, 4-17-1 Wakasato, Nagano, 380-8553, Japan
[b] Faculty of Engineering, Shinshu University, 4-17-1 Wakasato, Nagano, 380-8553, Japan
[c] Center for Energy and Environmental Science, Shinshu University, 4-17-1 Wakasato, Nagano, 380-8553, Japan

ARTICLE INFO

Keywords:
Silica
Titania
Adsorption
Photocatalysis
Photofuel cell

ABSTRACT

Silica nanolayers were formed as adsorbents on anatase-type titania particles immersed in tetraethyl orthosilicate (TEOS) solutions during UV irradiation. The concentration of the basic OH groups on the titania surface increased during the UV irradiation. The basicity promoted hydrolysis and subsequent polymerization of the TEOS on the titania surface on which the silica layers were deposited. The titania particles loading a small amount of the thin silica layers exhibited a higher photocatalytic activity for organic molecule degradation and photofuel cell performance than the original titania. The silica-modified titania particles efficiently adsorbed, then degraded the molecules on the surface. Therefore, the photocatalyzed surface modification in this study was significantly useful to activate the titania surface.

1. Introduction

Catalytic activity, adsorptivity, and connectivity of a material surface can be improved by surface modification. Such technologies are applicable to creating new functional materials and advancing the functions for developments in various fields. Effective adsorption, oxidation, and reduction are required for the photocatalytic degradation of organic molecules [1–5]. The adsorption is influenced by the properties of the photocatalyst surface, adsorbents coexisting with the photocatalysts, or photocatalyst-supports transporting the adsorbed molecules. One of the methods to perform the effective photocatalytic degradation is that the nanoparticles of the adsorbent were highly dispersed on the photocatalyst particle surface. In our previous study, the natural clay mineral, allophane, nanoparticles were dispersed on the titania particles by the sol–gel method using the allophane nanoparticle-dispersing titania sols [6–11]. Allophane has the smallest structural unit of all the natural clay minerals [12–17]. It is not easy that such particles having a very hydrophilic surface are dispersed in the sols due to their aggregation. There are methods to disperse the nanoparticles, which are physically separated during ultrasonic irradiation and electrostatistically charged for repulsion on the surface using some acids. The allophane enhanced the photocurrent in photofuel cells using titania electrodes by highly dispersing a small amount of allophane because the holes were efficiently consumed on the electrodes [7,8,10,11]. Photofuel cells, which are based on a photocatalytic reaction, generate electricity by the oxidative degradation of organic compounds. Such photocatalysis requires a facile adsorbent dispersion on the titania surface. It is reported that the concentration of basic OH groups increased on the titania surface during the UV irradiation, which is known as a superhydrophilicity effect of the photocatalysts [18]. This phenomenon can be utilized for the surface reaction of the modification. The photocatalytic reaction produces the active species on the surface. Previously, methylsiloxane monolayers adsorbed on the titania surface were transformed into silica by photoinduced oxidation [19]. The concentration of the species slowly increased because its efficiency is not very high during the photocatalytic reaction. This property is suitable to control the reaction forming very small particles or thin layers. Therefore, the photocatalyzed surface modification in the present study is significantly useful to advance the photocatalyst surface.

The adsorption ability of the titania photocatalyst can be improved by its surface modification in order to efficiently degrade organic molecules [20–22]. It is an effective method that the adsorbent nanoparticles are dispersed or the adsorbent nanolayers are formed on the titania surface. Silica as well as alumino silicates, such as allophane, is one of the adsorbents for organic molecules. In this study, the silica nanolayers were directly prepared on the titania particle surface by the sol–gel reaction of silicon alkoxide catalyzed by the photocatalytic activity of the titania. The organic dye degradation using the silica-modified titania particles and photoelectric conversion properties of the photofuel cells using the silica-modified titania electrodes were

* Corresponding author at: Department of Materials Chemistry, Faculty of Engineering, Shinshu University, 4-17-1 Wakasato, Nagano, 380-8553, Japan.
E-mail address: nishiki@shinshu-u.ac.jp (H. Nishikiori).

https://doi.org/10.1016/j.apcatb.2018.09.046
Received 24 May 2018; Received in revised form 12 September 2018; Accepted 16 September 2018
Available online 17 September 2018
0926-3373/

investigated in order to evaluate their photocatalytic activity.

2. Experimental section

2.1. Materials

Titania powder (Aerosil AEROXIDE TiO_2 P25) was used without further purification. Titanium tetraisopropoxide, TEOS, ethanol, nitric acid, hydrochloric acid, sodium hydroxide, methylene blue trihydrate, and starch (Wako, S or reagent grade) were used without further purification. Water was ion-exchanged and distilled using a distiller (Yamato WG23). The glass plates (Matsunami S-1111) and glass plates with FTO films (AGC Fabritech, 14 Ω cm^{-2}) were individually washed with a detergent and acetone, soaked in 0.10 mol dm^{-3} hydrochloric acid for 2 h, and washed with ethanol.

2.2. Sample preparation

The glass and FTO glass substrates were coated with a very thin titania film by the sol–gel method. The titania sol was prepared by mixing 25.0 cm^3 of ethanol, 0.21 cm^3 of nitric acid, and 0.21 cm^3 of water, then adding 5.00 cm^3 of titanium tetraisopropoxide in a dry nitrogen atmosphere. The anatase-type titania films were prepared by three or ten dip-coatings using the sol, then heating at 773 K for 30 min. The thickness of the ten-layered film was ca. 300 nm.

The titania powder was stirred and the substrates were immersed without stirring in 20 cm^3 of the 5, 10, 50, and 100 vol% ethanol solutions of TEOS in the dark or during light irradiation using a high-pressure mercury lamp (SEN LIGHTS HB-100-A, 100 W). The distance between the substrate and lamp was ca. 2 cm. After the irradiation for 10 min or 3 h, the samples were washed with ethanol, then dried at 337 K.

The silica sol was prepared by mixing 5.25 cm^3 of ethanol, 5.00 cm^3 of TEOS, and 1.65 cm^3 of 1.00 mmol dm^{-3} hydrochloric acid as the catalyst in the air. This solution was stirred during the addition, thoroughly stirred for an additional 5 min, then kept in a thermostated oven at 60 °C for 3 days. The resulting gel was ground to powder in mortars.

2.3. Measurements

A micromorphology study of the samples was done using a field emission scanning electron microscope (FE-SEM, Hitachi SU8000), scanning transmission electron microscope (STEM, Hitachi HD-2300 A), and transmission electron microscope (TEM, JEOL JEM-2010). The elemental mapping was conducted by the STEM. The X-ray diffraction (XRD) patterns were obtained during CuK_α irrradiation using an X-ray diffractometer (Rigaku SmartLab). The UV–vis absorption spectra were measured using a spectrophotometer (Shimadzu UV-3150). The Fourier transform infrared–reflection absorption spectroscopy (FTIR–RAS) for the film samples was conducted using an FTIR spectrophotometer (Shimadzu IRPrestige-21) with an RAS accessory. The X-ray photoelectron spectroscopy (XPS) was conducted by AlKα radiation of a 100 μm^2 area using an X-ray photoelectron spectrophotometer (JEOL JPS-9010MX). The pass energy was held at 55 eV. The elemental composition was also analyzed by the X-ray photoelectron spectrophotometer. The specific surface areas of the powder samples were estimated by the BET (Brunauer–Emmett–Teller) method from the adsorption isotherms of nitrogen gas using a volumetric gas adsorption instrument (BEL Japan, BELSORP-mini).

For examination of the photocatalytic properties, 50.0 mg of the photocatalyst powder samples were added to 40.0 cm^3 of 2.00 × 10^{-5} mol dm^{-3} aqueous solutions of methylene blue and 20.0 cm^3 of the aqueous solutions containing 0.20 mol dm^{-3} of sodium hydroxide with 0.250 *g* of starch. The suspensions were agitated in a glass beaker in the dark for 24 h and during the near-UV light irradiation (300–400 nm, peak at 352 nm, 40 μW cm^{-2}) from two 4-W black light bulbs (Toshiba FL4BLB). The UV–vis absorption spectra of the methylene blue in the centrifuged solutions were obtained as a function of the light irradiation time using the spectrophotometer. The FTIR spectra of the starch solutions were observed as a function of the irradiation time using the FTIR spectrophotometer with an attenuated total reflection (ATR) accessory and a ZnSe prism in order to evaluate the changes in the concentrations of the starch and the products as previously reported [11].

For examination of the properties of the photofuel cell electrodes, 20.0 cm^3 of the aqueous electrolyte solutions containing 0.20 mol dm^{-3} of sodium hydroxide with and without 0.250 g of starch were allowed to soak into the space between the sample and counter Pt electrodes. The distance between the two electrodes was adjusted to ca. 1.0 mm using a spacer. The samples were irradiated using monochromatic light generated by a fluorescence spectrophotometer (Shimadzu RF-5300) equipped with a Xe short arc lamp. During the light irradiation, the short circuit current was measured in the range from 350 to 400 nm by a digital multimeter (ADC 7461 A). The *J–V* curves of the electrodes were measured by a potentiostat (Hokuto Denko HSV-100) during the irradiation of the Xe short arc lamp. The intensity at each wavelength of the light source was obtained using a power meter (Molectron PM500 A) in order to estimate the incident photon-to-current conversion efficiency (IPCE) and quantum efficiency for the photocurrent from the excited ligands, i.e., the absorbed photon-to-current quantum efficiency (APCE), in the electrode samples.

3. Results and discussion

3.1. Characterization of the silica-modified titania particles

Figure S1 shows the FTIR spectra of the powder and electrode samples prepared using 100 vol% TEOS in the dark and during UV irradiation. The band at around 800–400 cm^{-1} observed in all the powder samples can be assigned to the TiO stretching vibration of the titania [23–25]. The spectrum of the powder sample prepared using 100% TEOS during the UV irradiation for 3 h exhibited bands at 1250–1000 cm^{-1} due to the silica. The FTIR spectral bands of the silica were assigned to the Si − O stretching mode of the Si − O–Si (around 1100 and 790 cm^{-1}) and Si − OH (around 930 cm^{-1}) [19,26–28]. The bands at around 1200 and 1100 cm^{-1} can be assigned to the SiO stretching vibration. The stretching band of the Si − O–Ti was also observed at around 950 cm^{-1} [22,29]. Base on the FTIR analysis of the powder samples, the silica band was only slightly observed in the samples prepared using 100% TEOS in the dark for 3 h and during the UV irradiation for 10 min. The hydrolysis and polycondensation of TEOS were promoted on the titania surface by the photocatalytic reaction. The bands for the electrode samples were observed on the higher wavenumber side than those for the powder samples because they were analyzed by the FTIR–RAS method. The band at around 820 cm^{-1} for all the electrode samples can be assigned to the TiO stretching vibration. The bands at around 1210 and 1100 cm^{-1} can be assigned to the SiO stretching vibration. The silica band can be observed in only the electrode sample prepared using the 100% TEOS during the UV irradiation for 3 h due to the sensitivity of the FTIR–RAS.

The SEM images of the surface of the original titania powder sample and the sample prepared using 100% TEOS during the UV irradiation for 3 h are shown in Figure S2. The original titania films on the electrodes consisted of about 20-nm particles. The surface morphology after the UV irradiation for 3 h in 100% TEOS was not distinct from that of the original titania. Figure S3 shows the TEM images of the original titania powder and the powder sample prepared using 100% TEOS during the UV irradiation for 3 h. At first glance, the surface of the titania particles irradiated by the UV light was not significantly different from the original titania surface. However, the amorphous phase seemed to be on the surface of the titania particle with the crystal lattice fringe because the outline of the particle was not clear after the UV irradiation.

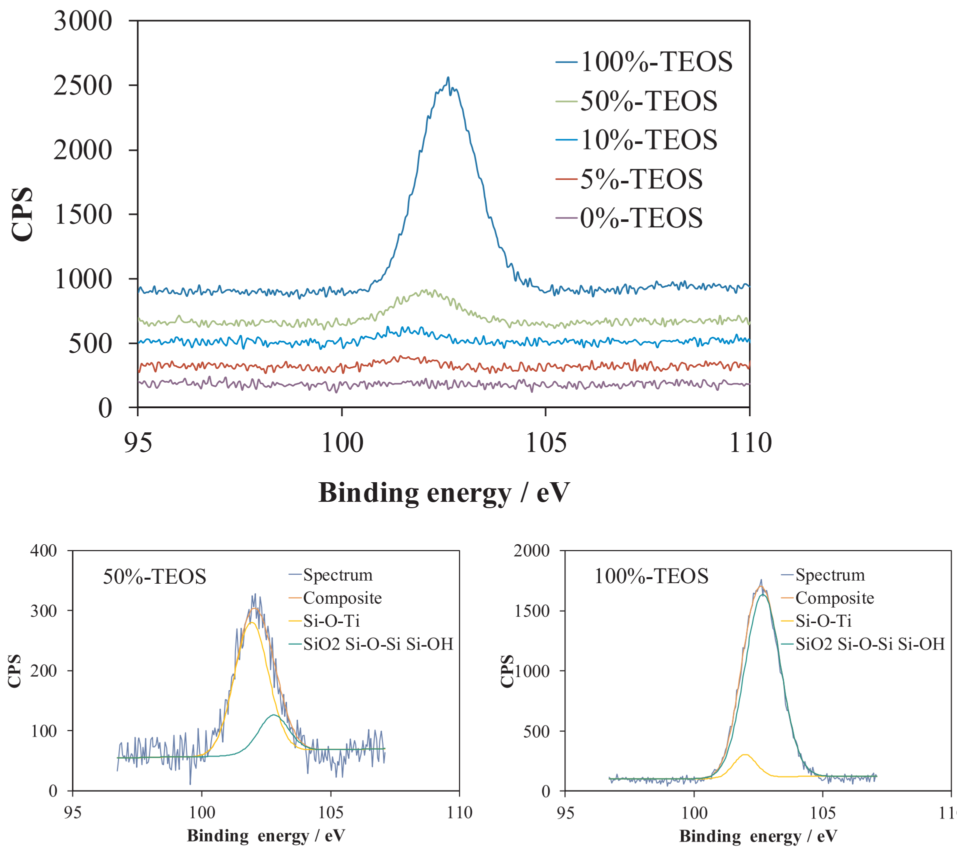

Fig. 1. XPS spectra related to the binding energy of the Si 2p electrons for the original titania powder and the powder samples prepared using the 5, 10, 50, and 100 vol% TEOS solutions during the UV irradiation for 10 min.

Table 1
Si/Ti ratio and peak binding energy of the powder samples prepared using the 5, 10, 50, and 100 vol% TEOS solutions during the UV irradiation for 10 min estimated from the XPS analysis.

TEOS vol%	5	10	50	100
Si/Ti ratio	< 0.4%	< 0.4%	5.4%	27.1%
Peak energy /eV	101.57	101.61	102.04	102.59

Relatively thick silica layers were formed on the titania under the above conditions. The lower concentrations of the TEOS solutions were used in order to prepare the nanaolayers on the titania. Fig. 1 shows the XPS spectra related to the binding energy of the Si 2p electrons for the original titania powder and the powder samples prepared using the 5, 10, 50, and 100 vol% TEOS solutions during the UV irradiation for 10 min. The peak energy was observed at around 101.6 eV in the samples prepared using the 5 and 10 vol% TEOS solutions. This binding energy was lower than that of the Si 2p electrons of the silica and can be assigned to the Si 2p electrons on the Si–O–Ti [19,20,29]. The peak was shifted to the higher energy side in the samples prepared using the 50 vol% TEOS solution and 100 vol% TEOS than in the sample prepared using the lower concentrated TEOS solutions. These spectra were separated into two components assigned to the electrons on the Si–O–Ti and the Si–O–Si/ Si – OH of the silica. The ratio of the electrons for the Si–O–Ti was higher in the sample prepared using the lower concentrated TEOS solution. Table 1 shows the Si/Ti ratio of each sample estimated from the XPS analysis. If it is postulated that a 20 nm-sized titania cubic particle is covered with a 0.1 nm-thick silica monolayer, the Si/Ti ratio of the titania particle loading the silica monolayer can be estimated to be about 3% by a simple calculation. The samples prepared using the 5 and 10 vol% TEOS solutions can load submonolayers of silica because their ratio values were less than 0.4%, which was much lower than the 3%.

Figure S4 shows the TEM images of the powder samples prepared using the 10 and 50 vol% TEOS solutions. No silica layer was clearly observed on the titania particles. Fig. 2 shows the elemental mapping images of the powder sample prepared using the 50 vol% TEOS solution by STEM. The mapping images of Si corresponded to those of Ti and O for the titania particle surface. This indicated that the silica was dispersed on the titania particle surface based on the resolution of the present images. These results indicated that the samples prepared using the 5 and 10 vol% TEOS solutions can load submonolayers of silica, which cannot be observed by TEM.

Figure S5 shows the UV–vis absorption spectra of the fluorescein adsorbed on the original titania sample and the silica-modified titania samples prepared using the 10 vol% TEOS solution and the 100 vol% TEOS compared to that of the fluorescein adsorbed on the silica gel powder. Fluorescein dye can be used as a pH probe molecule not only in solution, but also on the solid surface [30]. The anion and dianion species of fluorescein exhibited absorption peaks at 470 and 490 nm in water, respectively. The silica-modified titania particles prepared using the 100 vol% TEOS can be almost completely covered with the silica layer. Based on Ref. 30, the spectra of the dye adsorbed on the present silica and titania indicated the acidity corresponding to about pH 5.8 and 6.1 in water, respectively, estimated from the ratio of the dianion species to the anion species. The adsorption sites on the silica-modified titania samples prepared using the 10 vol% TEOS solution and the 100 vol% TEOS indicated the acidity corresponding to about pH 6.0 in water, intermediate between the values on the silica and titania. The silica did not necessarily cover all the surface of the titania particle even using the 100 vol% TEOS.

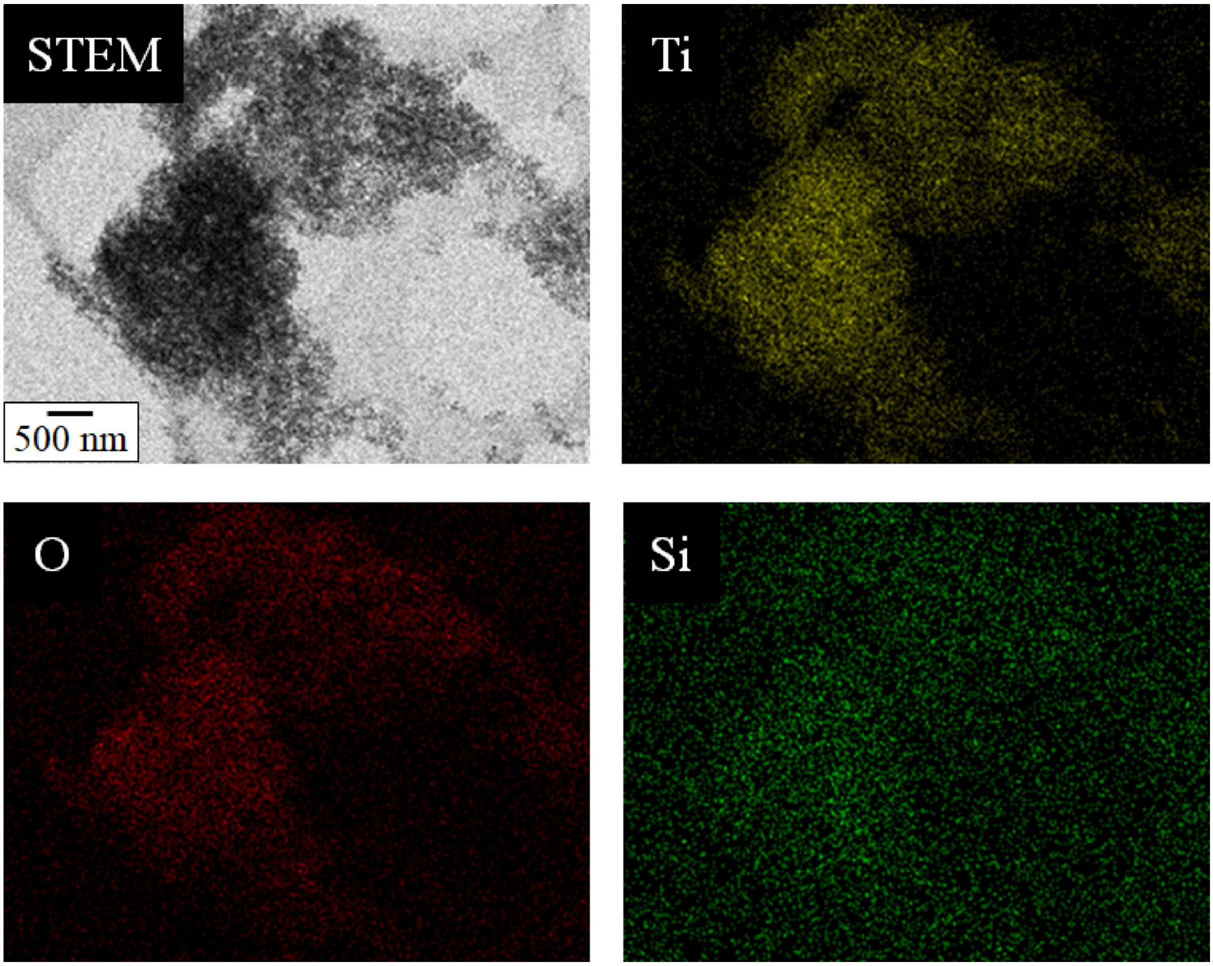

Fig. 2. Elemental mapping images of the powder sample prepared using the 50 vol% TEOS solution observed by STEM.

3.2. Photocatalytic activity of the silica-modified titania powders

Table 2 shows the BET specific surface area for the original titania and silica-modified titania powders. The specific surface area for the silica-modified titania powders prepared using the 5 and 10 vol% TEOS solutions was not significantly different from that for the original titania powder (49 $m^2 g^{-1}$). The specific surface area of the amorphous silica is expected to be much higher than that of the titania. The silica modification of the titania using the 100 vol% TEOS (Si/Ti = 27.1%) clearly increased its surface area by ca. 100% (96 $m^2 g^{-1}$). These results were similar to those in the previous study using the titania samples highly dispersing a small amount of allophane [8].

Fig. 3 shows the changes in the methylene blue concentration during the UV irradiation using the silica-modified titania powder samples and the quasi first-order reaction analysis of them. The concentration is normalized by each equilibrium concentration for the adsorption on the powder samples. The amounts of the methylene blue adsorbed in the dark were higher in the samples loading a higher amount of the silica as also shown in Fig. 3. The degradation rate constants of the samples prepared using the 5 and 10 vol% TEOS solutions were higher than that of the original titania [20–22]. These samples loaded the submonolayer silica, i.e., some areas of the titania particle surface can be bare. The layers much thicker than the monolayer should decrease the photocatalytic activity of the titania because the separated charges were difficult to transfer to the reactants adsorbed on the particle surface.

Fig. 4 shows the changes in the concentrations of starch (monomer unit) and the products, formic acid and CO_2, during the photocatalytic degradation of starch using the titania and silica-modified titania powders after each adsorption equilibrium. The amounts of the starch adsorbed on the original titania powder and the powder samples prepared using the 10 and 50 vol% TEOS solutions in the dark were 2.1, 2.4, and 2.9 mmol g^{-1}, respectively. They were higher in the samples loading a higher amount of the silica. The starch degradation and product formation rates on the samples prepared using the 10 vol% TEOS solution were higher than those on the other samples. Six times the amount of CO_2 than that of the monomer of the consumed starch should be produced from its oxidation. The change in the CO_2 concentration was lower than the amount expected from the decrease in the starch concentration. The partial oxidative products of starch, such as carboxy, carbonyl, and alcoholic compounds, should be easily adsorbed on the silica and titania surface. These results were similar to those in our previous study using the titania samples highly dispersing a small amount of allophane [8,11]. The photocatalytic activity of the samples corresponded to that for the methylene blue degradation.

Table 2
BET specific surface area of the powder samples prepared using the 0, 5, 10, 50, and 100 vol% TEOS solutions.

TEOS vol%	0	5	10	50	100
Specific surface area (/ $m^2 g^{-1}$)	49 ± 5	52 ± 3	56 ± 1	64 ± 6	96 ± 9

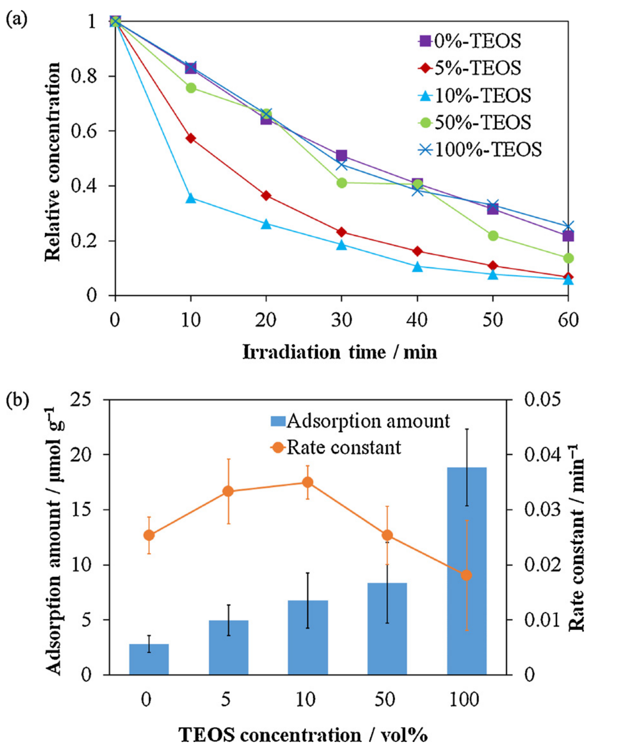

Fig. 3. (a) Changes in the methylene blue concentration during the UV irradiation using the original titania powder and the powder samples prepared using the 5, 10, 50, and 100 vol% TEOS solutions during the UV irradiation for 10 min, and (b) the amounts of the methylene blue adsorbed on the above samples in the dark for 24 h and the quasi first-order reaction rate constants of the methylene blue degradation using the above samples (For interpretation of the references to colour in this figure legend, the reader is referred to the web version of this article).

3.3. Photofuel cell performance of the silica-modified titania electrodes

Fig. 5 shows the photocurrent spectra of the titania electrode and the silica-modified titania electrodes observed in the electrolyte solution containing starch as a fuel. Table 3 shows the Si/Ti ratio of the electrode samples estimated by XPS. The values were higher than those of the powder samples shown in Table 1, because the surface layer of the film accessible to the TEOS solution was preferentially modified. The absorbed photon-to-current quantum efficiency was estimated as shown in Table 4. The short circuit photocurrent density values increased with an increase in the silica content up to the silica amount corresponding to its monolayer formed on the titania surface, then decreased in the electrolyte solutions with and without starch. A photocurrent was observed in the electrolyte solution without starch due to the water splitting. The photocatalytic degradation of the starch enhanced the photocurrent. Using the titania film prepared from the 10 vol% TEOS solution, the oxidative degradation of starch generated the highest amount of electricity during the UV irradiation. The charge transfer to the adsorbed water was also enhanced by the silica nanolayers. The titania films with a small amount of the silica nanolayers promoted degradation of the molecules and enhanced the photocurrent. The silica effectively adsorbed the molecules, the degradation of which efficiently consumed the holes. It is presumed that the charges can pass through the silica monolayer. Thicker silica layers should suppress the charge transfer to the reactants adsorbed on the particle surface. These results corresponded to our previous study using the titania electrodes highly dispersing a small amount of allophane, which enhanced the photocurrent in the photofuel cells [7,8,10,11]. In such systems, it is important that the adsorbent effectively adsorbs the fuel molecules, then transports them to the titania or transports the holes from the titania to the fuel molecules.

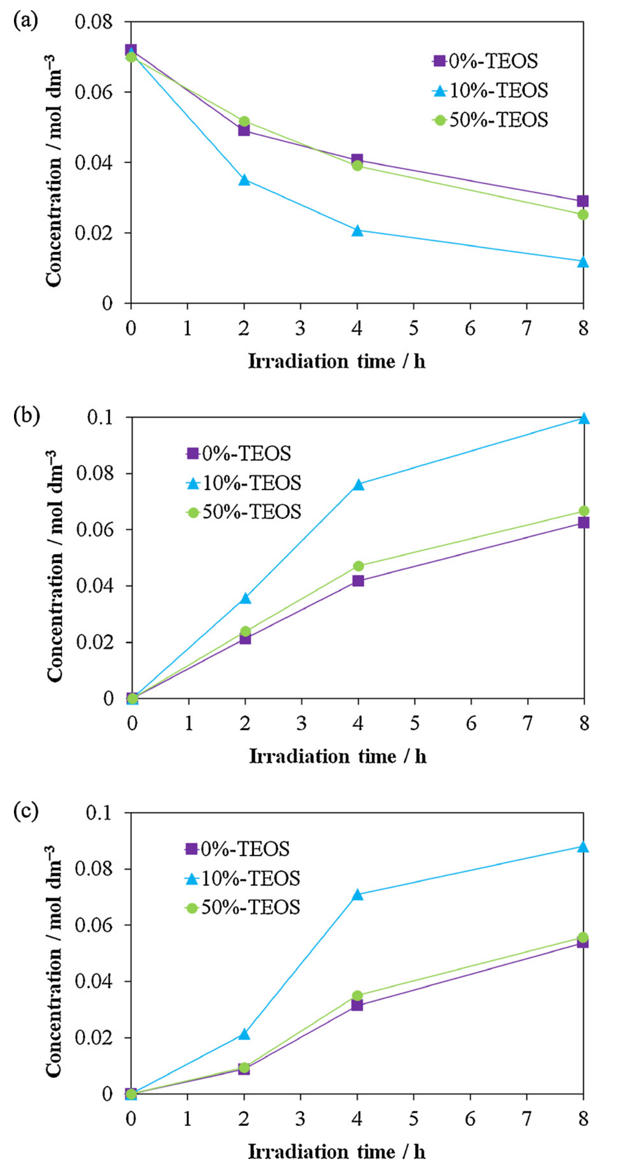

Fig. 4. Changes in the concentrations of (a) starch, (b) formic acid, and (c) CO_2 during the UV irradiation using the original titania powder and the powder samples prepared using the 10 and 50 vol% TEOS solutions during the UV irradiation for 10 min.

4. Conclusions

The silica nanolayers were prepared as an adsorbent on the titania particle surface by the sol–gel reaction of TEOS catalyzed by the photocatalytic activity of the titania during the UV irradiation. The concentration of the basic OH groups on the titania surface increased during the UV irradiation [18]. The basicity promoted the sol–gel reaction consisting of the hydrolysis and subsequent polymerization of TEOS on the titania surface, on which the silica layers were formed. The titania particles loading the silica submonolayers exhibited a higher photocatalytic activity for organic molecule degradation than the original titania. The silica submonolayers formed on the titania particle surface efficiently adsorbed, then degraded the molecules. Therefore, the photocatalyzed surface modification in this study is a promising method to advance the photocatalyst surface.

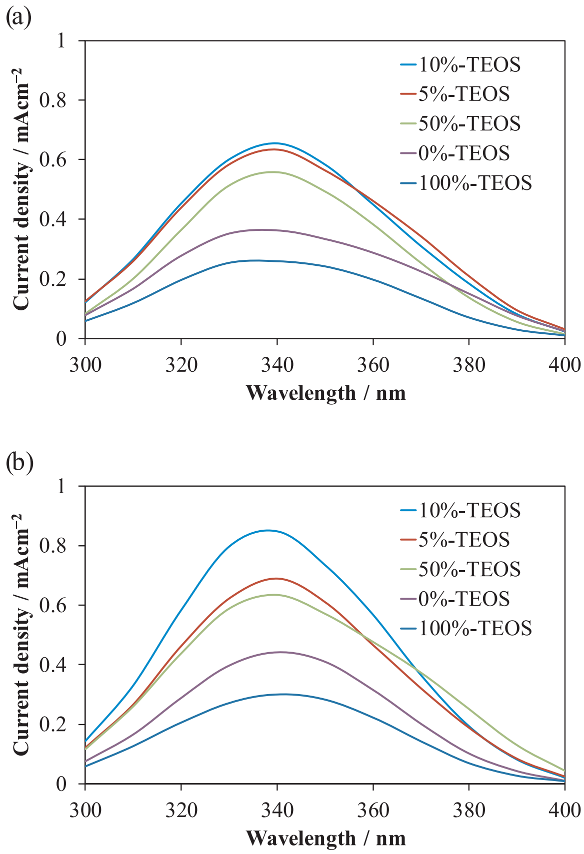

Fig. 5. Photocurrent spectra of the titania electrode and the silica-modified titania electrodes prepared using the 5, 10, 50, and 100 vol% TEOS solutions observed in the electrolyte solution (a) without and (b) with starch as a fuel.

Table 3
Si/Ti ratio of the electrode samples prepared using the 5, 10, 50, and 100 vol% TEOS solutions estimated by XPS.

TEOS vol%	5	10	50	100
Si/Ti ratio	0.7%	1.2%	12.8%	70.0%

Table 4
Absorbed photon-to-current quantum efficiency of the electrode samples prepared using the 5, 10, 50, and 100 vol% TEOS solutions observed in the electrolyte solution (a) without and (b) with starch.

TEOS vol%	5	10	50	100
a	7.9%	13.9%	14.4%	12.2%
b	9.7%	15.1%	18.6%	13.9%

Acknowledgement

This work was supported by JSPS KAKENHI Grant Numbers JP15K05472 and JP16KK0110.

Appendix A. Supplementary data

Supplementary material related to this article can be found, in the online version, at doi:https://doi.org/10.1016/j.apcatb.2018.09.046.

References

[1] H. Yoneyama, S. Haga, S. Yamanaka, Photocatalytic activities of microcrystalline titania incorporated in sheet silicates of clay, J. Phys. Chem. 93 (1989) 4833–4837.
[2] Y. Kitayama, T. Kodama, M. Abe, H. Shimotsuma, Y. Matsuda, Synthesis of titania pillared saponite in aqueous solution of acetic acid, J. Porous Mater. 5 (1998) 121–126.
[3] T. Tao, J.J. Yang, G.E. Maciel, Photoinduced decomposition of trichloroethylene on soil components, Environ. Sci. Technol. 33 (1999) 74–80.
[4] S. Suárez, J.M. Coronado, R. Portela, J.C. Martín, M. Yates, P. Avila, B. Sánchez, On the preparation of TiO_2 − sepiolite hybrid materials for the photocatalytic degradation of TCE: influence of TiO_2 distribution in the mineralization, Environ. Sci. Technol. 42 (2008) 5892–5896.
[5] T.L.R. Hewer, S. Suárez, J.M. Coronado, R. Portela, P. Avila, B. Sánchez, Hybrid photocatalysts for the degradation of trichloroethylene in air, Catal. Today 143 (2009) 302–308.
[6] H. Nishikiori, M. Furukawa, T. Fujii, Degradation of trichloroethylene using highly adsorptive allophane–TiO_2 nanocomposite, Appl. Catal. B-Environ. 102 (2011) 470–474.
[7] H. Nishikiori, M. Ito, R.A. Setiawan, A. Kikuchi, T. Yamakami, T. Fujii, Photofuel cells using allophane − titania nanocomposites, Chem. Lett. 41 (2012) 725–727.
[8] H. Nishikiori, S. Hashiguchi, M. Ito, R.A. Setiawan, T. Fujii, Reaction in photofuel cells using allophane–titania nanocomposite electrodes, Appl. Catal. B-Environ. 147 (2014) 246–250.
[9] H. Nishikiori, K. Morita, Y. Shibuya, K. Tagashira, Degradation of trichloroethylene using allophane–titania nanocomposite supported on porous filter, Chem. Lett. 44 (2015) 639–641.
[10] H. Nishikiori, S. Matsunaga, N. Furuichi, H. Takayama, K. Morita, K. Teshima, H. Yamashita, Influence of allophane distribution on photocatalytic activity of allophane–titania composite films, Appl. Clay Sci. 146 (2017) 43–49.
[11] H. Nishikiori, N. Furuichi, K. Teshima, H. Yamashita, Reaction kinetics on allophane–titania nanocomposite electrodes for photofuel cells, Chem. Lett. 46 (2017) 659–661.
[12] Y. Kitagawa, The “unit particle” of allophane, Am. Mineral. 56 (1971) 465–475.
[13] T. Henmi, K. Wada, Morphology and composition of allophane, Am. Mineral. 61 (1976) 379–390.
[14] S. Wada, K. Wada, Density and structure of allophane, Clay Miner. 12 (1977) 289–298.
[15] P.L. Hall, G.J. Churkman, B.K.G. Theng, Size distribution of allophane unit particles in aqueous suspensions, Clays Clay Miner. 33 (1985) 345–349.
[16] S.J. van der Gaast, K. Wada, S.-I. Wada, Y. Kakuto, Small-angle X-ray powder diffraction, morphology, and structure of allophane and imogolite, Clays Clay Miner. 33 (1985) 237–243.
[17] E. Hanudin, N. Matsue, T. Henmi, Adsorption of some low molecular weight organic acids on nano-ball allophane, Clay Sci. 11 (1999) 57–72.
[18] N. Sakai, A. Fujishima, T. Watanabe, K. Hashimoto, Quantitative evaluation of the photoinduced hydrophilic conversion properties of TiO_2 thin film surfaces by the reciprocal of contact angle, J. Phys. Chem. B 107 (2003) 1028–1035.
[19] H. Tada, Photoinduced oxidation of methylsiloxane monolayers chemisorbed on TiO_2, Langmuir 12 (1996) 966–971.
[20] M.S. Vohra, J.S. Lee, W.Y. Choi, Enhanced photocatalytic degradation of tetramethylammonium on silica-loaded titania, J. Appl. Electrochem. 35 (2005) 757–763.
[21] Y.Z. Li, S.J. Kim, Synthesis and characterization of nano titania particles embedded in mesoporous silica with both high photocatalytic activity and adsorption capability, J. Phys. Chem. B 109 (2005) 12309–12315.
[22] K. Gude, V.M. Gun'ko, J.P. Blitz, Adsorption and photocatalytic decomposition of methylene blue on surface modified silica and silica-titania, Colloids Surf. A: Physicochem. Eng. Aspects 325 (2008) 17–20.
[23] B.C. Trasferetti, C.U. Davanzo, R.A. Zoppi, N.C. da Cruz, M.A.B. de Moraes, Berreman effect applied to phase characterization of thin films supported on metallic substrates: The case of TiO_2, Phys. Rev. B 64 (2001) 125404-1–125404-8.
[24] B.C. Trasferetti, C.U. Davanzo, R.A. Zoppi, Infrared reflection-absorption characterization of TiO_2 films on ITO: detection of LO modes, Electrochem. Commun. 4 (2002) 301–304.
[25] C. Pecharromán, F. Gracía, J.P. Holgado, M. Ocaña, A.R. González-Elipe, J. Bassas, J. Santiso, A. Figueras, Determination of texture by infrared spectroscopy in titanium oxide–anatase thin films, J. Appl. Phys. 93 (2003) 4634–4645.
[26] A. Bertoluzza, C. Fagnona, M.A. Morelli, V. Gottardi, M. Guglielmi, Raman and infrared spectra on silica gel evolving toward glass, J. Non-Cryst. Solids 48 (1982) 117–128.
[27] Y. Abe, N. Sugimoto, Y. Nagao, T. Misono, Preparation of a gel-like silica glass by the condensation of silicic acid in organic solvents, Yogyo-Kyokai-Shi 95 (1987) 672–675.
[28] J.K. West, L.L. Hench, Molecular orbital models of silica rings and their vibrational spectra, J. Am. Ceram. Soc. 78 (1995) 1093–1096.
[29] L. Fang, L. Hou, Y. Zhang, Y. Wang, G. Yan, Synthesis of highly hydrophobic rutile titania-silica nanocomposites by an improved hydrolysis co-precipitation method, Ceram. Int. 43 (2017) 5592–5598.
[30] R. Sjöback, J. Nygren, M. Kubista, Absorption and fluorescence properties of fluorescein, Spectrochim. Acta A: Mol. Biomol. Spectrosc. 51 (1995) L7–L21.